



## Research Article

Yong-Sik Chu, Batmunkh Davaabal, Dae-Sung Kim, Sung-Kwan Seo, Yoo Kim, Claus Ruescher, and Jadambaa Temuujin\*

# Reactivity of fly ashes milled in different milling devices

<https://doi.org/10.1515/rams-2019-0028>

Received Jan 23, 2019; accepted Jul 24, 2019

**Abstract:** The effect of two different milling devices, namely attrition mill versus vibration mill, on the reactivity of fly ash was studied. High calcium fly ash from 4<sup>th</sup> Thermal power station of Ulaanbaatar (Mongolia) was used for the experiments. The raw and processed samples were characterized by XRD, SEM, Particle size distribution, BET, Blaine surface area and density measurements. The efficiency of 1 hour milling was evaluated with the Blaine surface area set to be more than 5000 cm<sup>2</sup>/g. The physical and chemical properties of the attrition milled fly ash changed not much compared to the vibration milled samples. For example the d<sub>50</sub> particle size became reduced from 29 μm to 6 μm by attrition milling and in vibration milled fly ash it was reduced to 7 μm. The density increased from 2.44 g/cm<sup>3</sup> of raw fly ash to 2.84 g/cm<sup>3</sup> and 2.79 g/cm<sup>3</sup> in attrition and vibration milled samples, respectively. Mechanical milling revealed not only a particle size reduction but also the formation of a denser microstructure. As a result the vibration milled fly ash showed a weaker interaction with the alkaline solution (8 M NaOH used here) compared to the attrition milled fly ash. Consequently, compressive strength of the binder prepared using the attrition milled fly ash was higher, 61 MPa, while for vibration milled fly ash it was 49 MPa. For comparison unmilled fly ash, it was 21 MPa.

**Keywords:** fly ash; milling; attrition mill; vibration mill; reactivity; geopolymer binder

**\*Corresponding Author: Jadambaa Temuujin:** Laboratory of Materials Science and Technology, Institute of Chemistry and Chemical Technology, Mongolian Academy of Sciences, Ulaanbaatar 51, Mongolia; Email: temuujin.mgl@gmail.com

**Yong-Sik Chu, Dae-Sung Kim, Sung-Kwan Seo, Yoo Kim:** Korea Institute of Ceramic Engineering and Technology, Jinju-si, Gyeongsangnam-do, Korea

**Batmunkh Davaabal:** Laboratory of Materials Science and Technology, Institute of Chemistry and Chemical Technology, Mongolian Academy of Sciences, Ulaanbaatar 51, Mongolia

**Claus Ruescher:** Institute of Mineralogy, Leibniz University of Hannover, Hannover, Germany

## 1 Introduction

The modern society encounters serious problems concerning huge volume of wastes accumulated by everyday needs of humanity. One type of wastes is fly ash released from power stations of coal combustion. It is the fifth largest amount of solid wastes in the world, accounting for up to 750 million tons per year [1–3]. Fly ashes represent a mixture of amorphous and crystalline components with a complex microstructure. The shape of fly ash dust represents mostly microspheres with presence of some irregular particles. The utilization of fly ash is given a high attention due to its favourable properties for using as a concrete additive. Generally fly ashes are used as concrete additive in advance for their particle shape (ball bearing effect) or due to their pozzolonic or hydraulic reaction. Fly ashes have been used for the production of cement, asbestos, brick, concrete, embankments, road construction, mine reclamation, extraction of valuable metals, and production of ceramic and glass ceramic, zeolite synthesis, adsorbents and geopolymers [2, 3].

Geopolymers, known as inorganic polymers, are binders that develop strength at ambient to moderate high temperatures and have found applications as environmentally friendly building materials [4, 5]. The “geopolymerization” process includes the reaction of the aluminosilicate phase of fly ash with the alkaline liquid, sometimes also called alkali activation, forming monomers which further polycondensate and cross link to form a polysiloxo/polysialate network. This amorphous cross linked network gives the main contribution to the benefiting mechanical properties of geopolymer materials. The important effect to consider is the reaction of certain fly ash components with the alkaline liquid. As said fly ash constitutes contain amorphous aluminosilicates and crystalline phases. It is known that only the amorphous part of the fly ash represents the reactive part which is prone to become dissolved by alkaline solution. Therefore, an increased reactivity of the amorphous part, e.g. by reduction of particle size, should lead to an improved geopolymerisation reaction within the mixture. A surface modification



of the crystalline phases could support its embedding in the geopolymer for a higher mechanical strength, too.

Generally, mechanical milling induces physical changes of the powders and increases the reactivity [6]. However, physical changes are not always accompanied by reactivity. Reactivity should be accompanied by physical changes such as dislocation, stress and strain of the crystalline lattice of crystalline components, decrease in particle sizes, increase of internal and surface energy, increase the surface area and decrease of the cohesive energy of solids [7]. Influence of mechanical activation of fly ash on geopolymer materials preparation cured at elevated or ambient temperature has been described previously [8–10]. In the previous reports the influence of milling device type on the physical properties of the activated fly ash and consequently geopolymers prepared from these fly ashes have been studied [8, 9]. There are different type of milling devices used for industrial and research purposes such as vibration mill, attrition mill, mixer mill and planetary mill. Vibration mill and attrition mills are often used for industrial practice. More detailed explanation of working principle of the attrition and vibration mills is given by Balaz [11]. The main advantage of the attrition mill is power input is used directly to agitating media to achieve milling, while for the vibration mill uses impact of the milling media developed by the milling chamber by rotation of out-of-balance weights. Kumar *et al.* [6] have noted that milling of fly ash with vibratory mill improves the reactivity more than that of the attrition milled fly ash [7–9]. Balaz suggested that with attrition milling specifically the surface area would be increased, but the crystallinity remains unaltered or becomes reduced much less than by vibration milling [12]. In the attrition mill the main milling impact occurs via shear while in the vibration mill via impact force. But in fact, the milling effects may hard to be compared to each other, unless it is assured that the same constraints are controlled, *i.e.* samples, milling time, temperature. Kumar *et al.* [6] have used for geopolymers binder preparation approximately the same particle size of fly ashes ground by attrition and vibration mills. They observed that there is no clear correlation between the fly ash particle size, geopolymerization reaction rate and reactivity induced by milling. The geopolymerization reaction product shows the main effect on compact microstructure. These authors showed that vibration milled fly ash has higher reactivity than attrition milled fly ash toward alkali activation. On the other hand, Mucsi *et al.* [13] observed higher mechanical properties and reactivity for the low calcium land filled fly ash milled by stirred media mill (same milling effect with the attrition mill). A finer particle size obtained by stirred milling combined with the filler

effect of the fine particle size is assumed to be the main reason for this behaviour. Such discrepancy of attrition milling impacts is not known. Generally land filled ash differs from the fly ash by their physicochemical, surface properties and particle size distribution [14]. Differences of the raw materials properties may show influence on reactivity of milled fly ash with the various milling devices. Therefore, it is important to study the milling impacts on fly ash rather than on land filled ash to verify effects of milling devices on final geopolymer properties.

In this paper we have performed milling with the attrition and vibration mill observing that each mill has a different milling effect. The Blaine surface area of the milled fly ash was determined in order to control the surface reactivity induced by the milling process. The mechanical strengths of the geopolymeric materials prepared from the fly ash samples with an approximate same surface area were evaluated for efficiency of the milling.

## 2 Materials and Methods

### 2.1 Material

Fly ash from 4<sup>th</sup> Thermal power station of Ulaanbaatar city was used as raw material. This thermal power station uses coals from Baganuur and Shivee ovoo deposits. The fly ash produced was supplied separately to concrete manufacturers. However, since 2017, the power station uses preliminary mixed and fine ground coals for the fuel source, whereas previously both types of coals were used separately. In a previous work the two types of fly ashes related to the two types of coals could be characterized separately and used for preparation of geopolymers [15]. In this work it is the first time using fly ash obtained by burning of the Baganuur and Shivee ovoo mixed coals. Therefore, the chemical and mineralogical composition of the present fly ash should tend to give some average values compared to the earlier data [15], but could also deviate due to the changes in composition of the natural material. The chemical composition of the raw materials used in this work is listed in Table 1. The contents of the main oxides were somewhat between Baganuur and Shivee ovoo fly ashes [15] obtained earlier. The calcium oxide content was lower than that of average of the 2 fly ashes.

The XRD patterns showed (see below, Figure 7) that the raw fly ash contains magnetite-Fe<sub>3</sub>O<sub>4</sub>, Gehlenite-Ca<sub>2</sub>Al(AlSiO<sub>7</sub>), Quartz-SiO<sub>2</sub>, Hematite-Fe<sub>2</sub>O<sub>3</sub>, Calcium sulfate-CaSO<sub>4</sub>; Akermanite-Ca<sub>2</sub>Mg(Si<sub>2</sub>O<sub>7</sub>). The mineralogical composition of the raw fly ash compromises the re-

**Table 1:** The chemical compositions of the used raw fly ash.

	SiO <sub>2</sub>	Al <sub>2</sub> O <sub>3</sub>	Na <sub>2</sub> O	Fe <sub>2</sub> O <sub>3</sub>	K <sub>2</sub> O	CaO	MgO	SO <sub>3</sub>	TiO <sub>2</sub>	LOI
Raw fly ash	47.82	14.87	0.24	11.90	0.91	16.03	3.16	1.31	0.72	1.33

sults obtained earlier for the Baganuur and Shivee ovoov fly ashes [15].

The radium equivalent activity of fly ash was 575.3 Bq/kg which is higher than the critical value given previously (370 Bq/kg) [16, 17]. According to the radium equivalent activity this fly ash cannot be used as building materials [17]. But fly ash is itself not the building material such as geopolymers. It's one of the raw materials used for making geopolymer concretes and mortars. Radiation value as 1300 Bq/kg can be reduced substantially to 280 Bq/kg by adding aggregates into mixture geopolymer paste [15]. Therefore the present fly ash should not be considered as a harmful compound for the building materials application.

## 2.2 Methods

Milling was performed with attrition and vibration mills. The milling was performed with the vibration mill from Woojin Precision Co., Ltd. (Korea) using the steel balls as supplied in the specially designed sample container made of steel, too. The ball and container are made of hardened steel. The diameter of the sample container is about 20 cm and the height is about 24 cm of elliptical shape. The size of the steel ball was 1.27 cm and the weight of the balls was about 20 kg. The filling rate of the grinding media is about 70% of the volume of the sample container. The rotation speed of the mill was 1750 rpm. Typically 1 kg fly ash was used for the milling and the milling time was 1 h. After milling the Blaine surface area was measured which was 5900 cm<sup>2</sup>/g.

The attrition mill HAS-1 from Union Process Co. was used. Attrition mill has a grinding volume with 5 L. Grinding media was hardened steel with 1 cm diameter. In order to obtain fly ash samples with Blaine surface area of 5000-6000 cm<sup>2</sup>/g the fly ash samples were milled by steel ball with a batch method. With a trial and error method by changing the ball: fly ash ratio a Blaine surface area of 5200 cm<sup>2</sup>/g was obtained. For this procedure the optimal milling regime was: weight of balls 3400 g, weight of fly ash 850 g and milling time 1 h.

The geopolymers were prepared in series using the 8M NaOH solution as alkaline activator. In order to have a uniform consistency for the raw fly ash, 36 mL of sodium hydroxide solution was used. For the milled fly ashes 40

mL of sodium hydroxide solutions was added. The solutions were added into 100 g of solids and then hand mixed until the uniform consistency was reached. The liquid to Solid (L/S) ratio was 0.37 for raw fly ash, 0.41 for attrition milled fly ash, and 0.4 for vibration milled fly ash. The mixtures were poured into cubic moulds with edge of 20 mm. The moulds were wrapped with a plastic bag and placed into an oven at 70°C temperature and cured for 24 h. The moulds were removed from the oven and de-wrapped and de-moulded.

## 3 Characterization

X-ray diffraction (XRD) were carried out using an X-ray diffractometer (Shimadzu MAXima-X XRD-7000). XRF analyses were obtained using a wavelength dispersive X-ray fluorescence spectrometer (PANalytical Axios).

Blaine surface area was determined by the air-permeability test (PSH-2) as used for characterization of the fineness of a cement powder. Further on the raw and milled fly ash samples were characterized by their changes in particle size and density. The particle sizes were determined by a particle size analyzer (Horiba LA950). The density of the powders was determined using an automatic pycnometer (Micromeritics AccuPyc 1330) with 10 measurements being made on each sample. BET measurements were performed with a Micromeritics Tristar 3000 BET analyzer. Samples were outgassed at 200°C for 6 h. TG measurements were carried out with a DTA-TG instrument (Hitachi, DTA/TG 7300). Approximately 10 mg of fly ash samples were used for heating measurements up to 1150°C at a heating rate of 10°C/min in air.

The FTIR measurements carried out on raw and milled fly ashes with a Shimadzu FTIR 8200PC spectrometer by using KBr suspended disc method.

The fly ashes and alkali-activated products were characterized by SEM (Topcon SM-300 electron microscope operated at 20 kV). The compressive strengths of the 2 cm edge cubes were determined at least on four samples of each composition after curing for 7 days, using a Jinan WDW-50 universal testing machine. For compressive strength data an average of 4 measurements was used. Water absorption was measured by the weight difference per-

centage of the raw and boiling water-saturated samples. Bulk density was measured by weight and volume ratio of the cube specimens. For water absorption and bulk density data an average of at least 2 measurements was used. Samples are denoted as Raw-FA, AM-FA, VM-FA which indicate raw, attrition and vibration milled fly ashes in the following.

## 4 Results and Discussion

### 4.1 Effect of mechanical activation on the physical-chemical properties of the fly ash

Blaine surface area, density and particle size ( $D_{50}$ ) of the raw fly ash, and fly ash milled with vibration and attrition mills are given in Table 2.

**Table 2:** Physical properties change of milled fly ashes

Ash	Blaine surface area, $\text{cm}^2/\text{g}$	Density, $\text{g}/\text{cm}^3$	$D_{50}$ , $\mu\text{m}$
Raw-FA	2750	2.44	28.9
AM-FA	5200	2.84	6.25
VM-FA	5900	2.79	7.25

Both milled fly ashes show a significantly higher density compared to the raw fly ash. A similar behaviour was also observed during grinding of the pond ash [14]. This effect could be related to a decrease of the particle size, *i.e.* the volume of the particles, with a loss of pore volume due to fractionation and/or a compaction revealing a decrease in pore volume. It may be noted that the Blaine surface area of the vibration milled fly ash was a bit higher than for the attrition milled fly ash. The cumulative particle size distribution of the raw and milled fly ashes is shown in Figure 1. There is a significant reduction in the particle size  $D_{50}$  values observing 6.25  $\mu\text{m}$  and 7.25  $\mu\text{m}$  for attrition and vibration milling, respectively, compared to the raw fly ash (28.9  $\mu\text{m}$ , Table 3). However, pronounced more intensity is observed for the attrition milled fly ash towards smaller particles sizes compared to the vibration milled sample.

The XRD patterns of the milled fly ashes were almost the same as raw fly ash shown in Figure 7 and, therefore, not shown here. Interestingly certain XRD peaks intensity of the quartz in the milled fly ashes were a bit sharper than in the raw fly ash. The fly ash represents a heterogeneous system with a mixture of the crystalline and amorphous

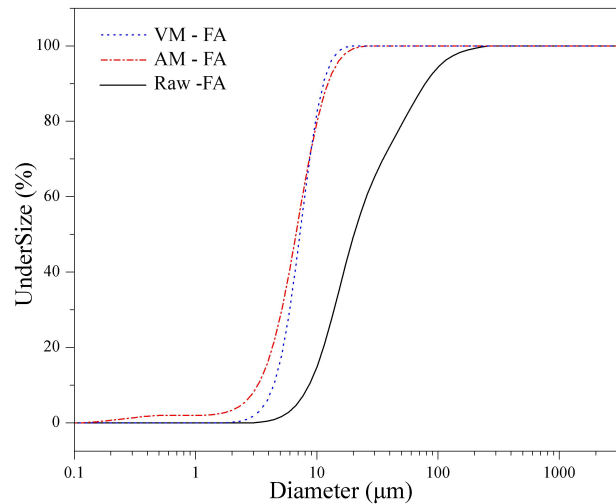


**Figure 1:** Particle size distribution of the raw and milled fly ashes.

constituents. Likely, during milling a release of the crystalline part from the embedded glassy structure occurred.

Figure 2 shows SEM micrographs of the raw and milled fly ashes. The raw sample showed mainly spherical particles. It is also observed that there is a higher contribution of much finer particles in the milled samples and only little difference in particle shape between attrition and vibration milled fly ashes.

Figure 3 shows the results of TG-loss of the raw and milled fly ashes, which were kept in a plastic bag before the TG experiment. Samples were measured without any pre-treatment. The TG measurements indicate that the total weight loss of vibration milled fly ash is higher than those of the raw and attrition milled fly ashes. The weight loss observed between 100°C and 300°C in the milled fly ash is caused by adsorbed moisture which is not present in the unmilled raw fly ash. This indicates that there occurs an additional adsorption due to surface activation. All samples show a weight loss between 450 and 650°C which is most pronounced in the vibration milled fly ash. The steep weight loss in the fly ashes from 450°C to 650°C could be related to unburnt carbon [18]. The higher weight loss in vibration milled fly ash represents an interesting phenomenon and could indicate the loss of additional hydroxyl groups present on the surface of fly ash or unburnt carbon. According to this, especially by vibration milling lead to a structural change which caused adsorption of some hydroxyl groups on the surface of fly ash/unburnt carbon. The thermal weight loss caused by dehydroxylation in the raw fly ash was 0.3%, but it increases to 1.2% in the vibration milled sample. The total weight loss of the raw fly ash is around 0.6% which is lower than the Loss on



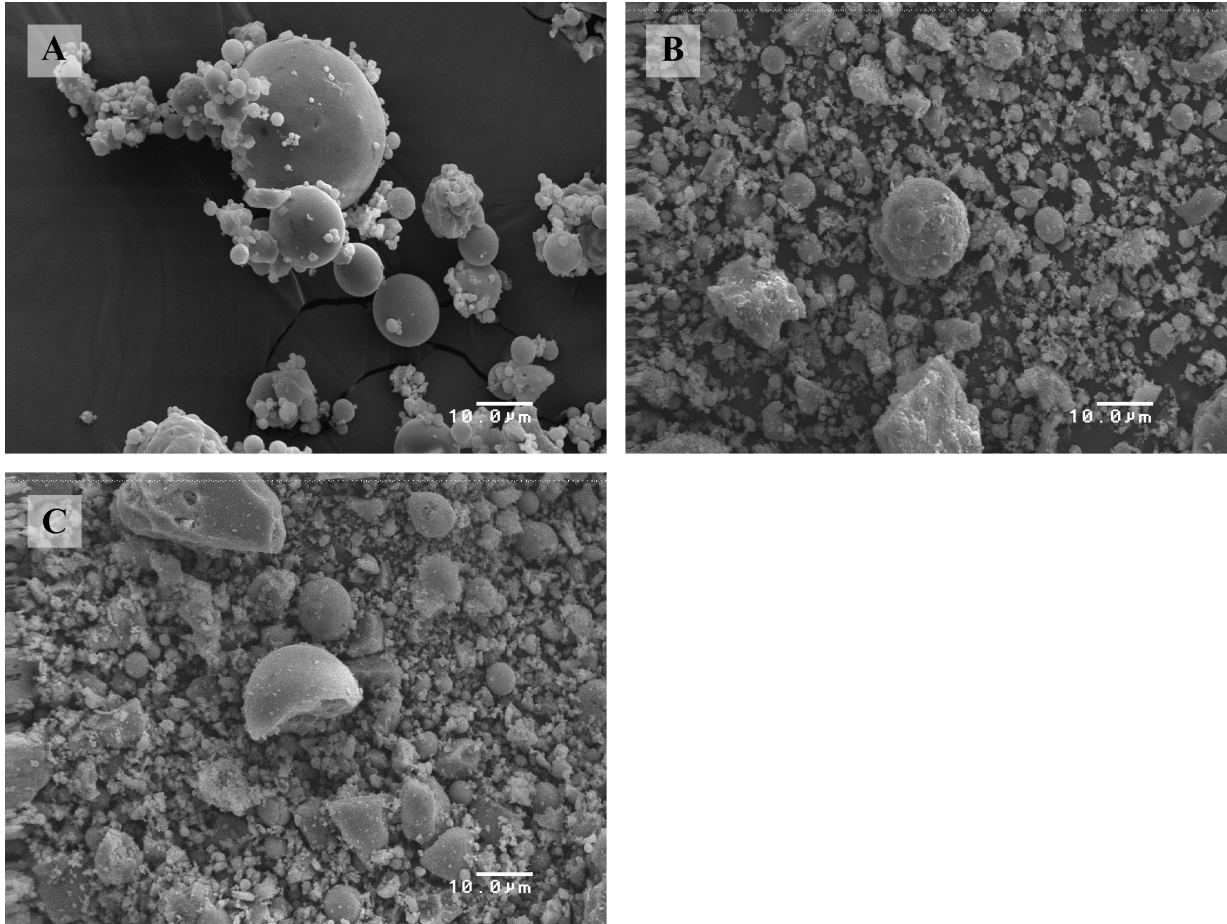


Figure 2: SEM micrographs of the raw (A), vibration (B) and attrition (C) milled fly ashes.

Ignition data shown in the Table 1. The origin of weight loss of all samples that occurred after 970°C is related to desulfurization. All samples show a weight gain from 700°C up to 950°C caused by oxidation of iron.

Figure 4 shows FTIR spectra of the raw and milled fly ashes. The raw fly ash shows a rather broad band with a peak centred at 1096  $\text{cm}^{-1}$ . This band together with further peaks observed with maxima at 780  $\text{cm}^{-1}$  and 460  $\text{cm}^{-1}$  are attributed to Si-O vibrations, which are related mainly to amorphous  $\text{SiO}_2$ . The broad peak with maximum at about 3437  $\text{cm}^{-1}$  typically comprises the symmetric and asymmetric O-H stretch vibrations. The peak at 1630  $\text{cm}^{-1}$  corresponds to the bending vibration of water molecules. The absorption band at 690  $\text{cm}^{-1}$  could be assigned to quartz which may overlap with the anhydrite which appears at 679  $\text{cm}^{-1}$  [19]. The presence of anhydrite is supported by XRD pattern of fly ash (Figure 7). With milling this band split into 2 bands at 680 and 690  $\text{cm}^{-1}$  due to quartz and anhydrite. For the milled fly ash samples, the spectra show all features described for the raw fly ash with somehow more pronounced intensities. This

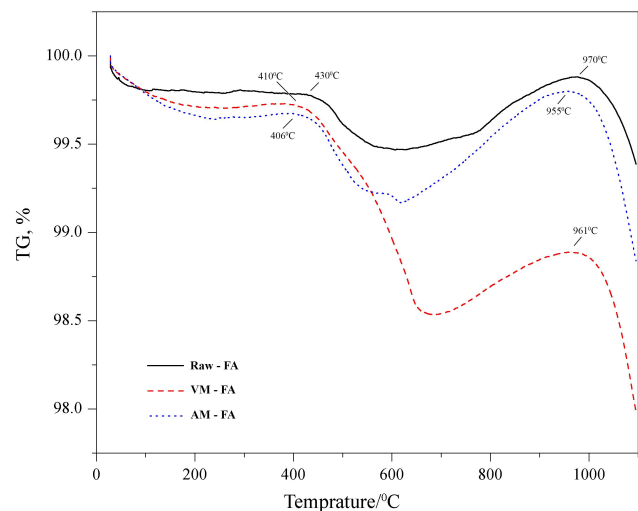


Figure 3: TG of the raw and milled fly ashes.

could be explained by the more homogeneous distribution of the milled material in the KBr matrix. For example the peak with maximum at 796  $\text{cm}^{-1}$  shows a low wavenumber

**Table 3:** Physical and mechanical properties of geopolymers prepared from raw and milled fly ashes.

Ash used for geopolymers	BET, m <sup>2</sup> /g	Density, g/cm <sup>3</sup>	Compressive strength, MPa	Water absorption, %	Bulk density, g/cm <sup>3</sup>
Raw-FA	11.61	2.49	21.3 (1.97)	16.50 (1.33)	1.48 (0.01)
AM-FA	20.47	2.41	60.56 (2.55)	10.58 (1.42)	1.68 (0.03)
VM-FA	17.8	2.39	49.53 (2.59)	14.94 (1.1)	1.58 (0.01)

(Values in brackets indicate the standard deviation of repeated measurements.)

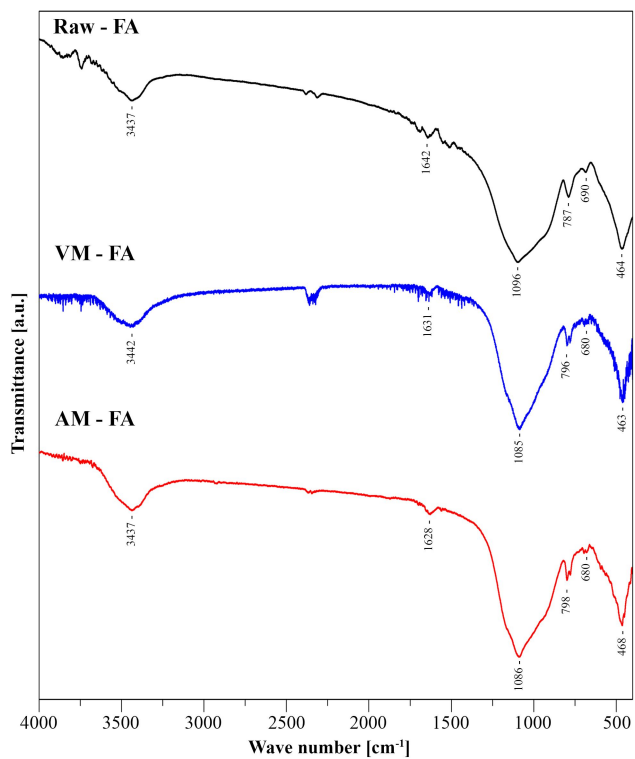


**Figure 4:** FTIR spectra of the raw, vibration and attrition milled fly ashes.

shoulder in the milled samples, which indicates the presence of quartz. The presence of characteristic quartz doublet at 796 and 780 cm<sup>-1</sup> in the milled fly ashes indicate that the release of quartz crystals embedded in a glassy phase in these samples have occurred.

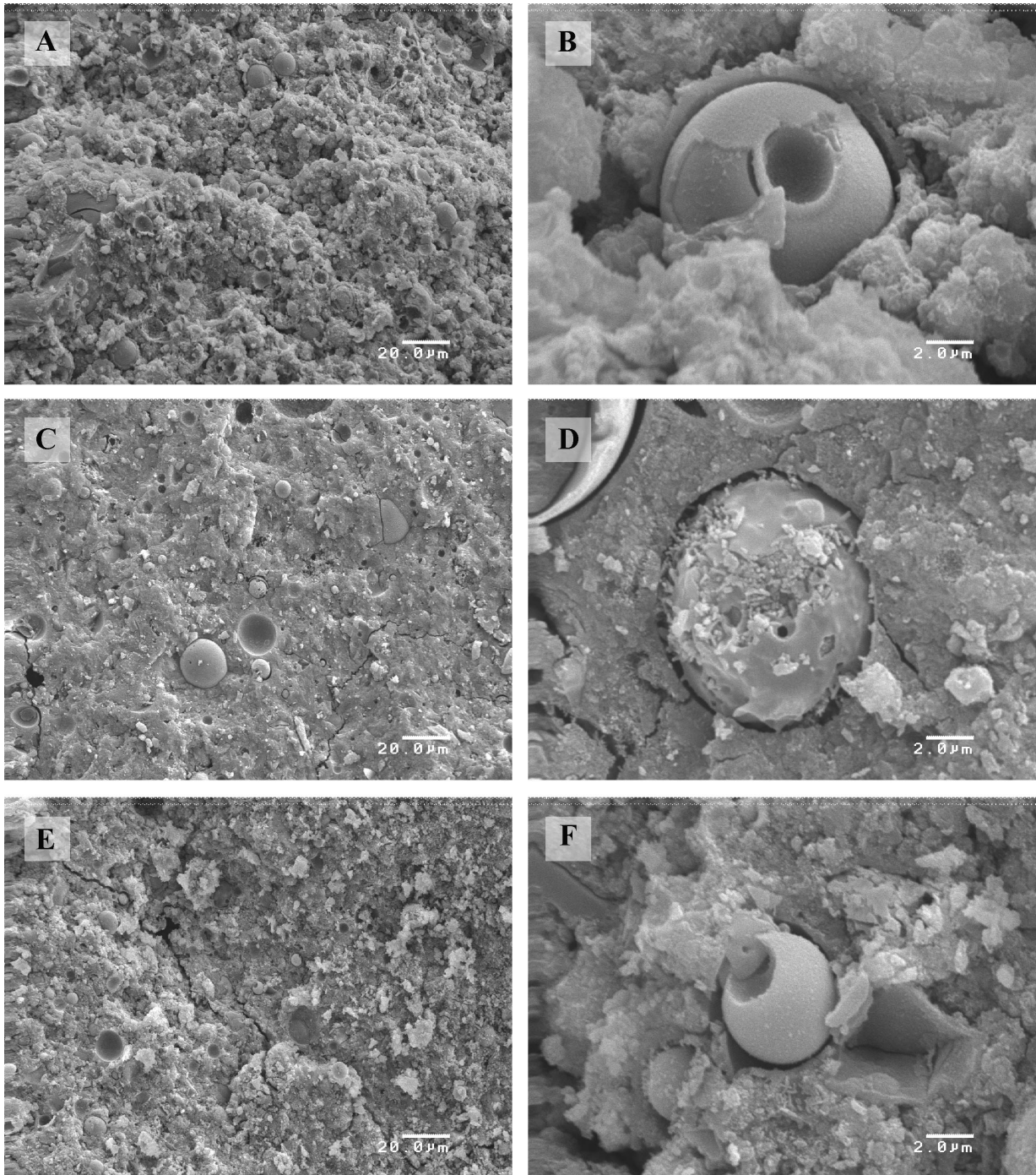
## 4.2 Geopolymers prepared from fly ashes activated with various milling devices

Table 3 collects the physical and mechanical properties of geopolymers prepared from fly ash milled by various devices.

It is obtained that the mechanical activation improves the compressive strength of the geopolymers. Milling with the attrition mill improved the compressive strength of

the geopolymers by about 20% more compared to the vibration milled related geopolymer. Water absorption and density data also supports the trend observed in the compressive strength values. Although, the differences of the average particle sizes and densities between the attrition milled and vibration milled samples are small, the mechanical properties differ substantially. The BET specific surface area of the attrition milled fly ash based geopolymer is the highest, higher by a factor of 1.76 compared to the raw fly ash related geopolymer. For comparison the BET specific surface area for the vibration milled fly ash related geopolymer is enhanced by a factor 1.53. The relative increase in BET values could be directly related to the increase in compressive strength values. It is known that for the same type of ceramics the compressive strength decreases with increase in porosity [20–22]. In the present case it shows an opposite trend. It can be explained with the nature of geopolymer structure. The geopolymer microstructure consists of amorphous gel forming a three-dimensional network with cavities similar to a zeolite type with the micropores occupied by water [23]. Therefore, it can be suggested that a higher BET surface area indicates a higher rate of geopolymeric gel revealing a high compressive strength value. A lower water sorption at higher BET surface area is related with the nature of the porosity. In the milled fly ash based geopolymers isolated pores may become more likely while the raw fly ash based geopolymer contains more interconnected pores. Geopolymer specimens based on both milled ashes show enhanced compressive strength than raw fly ash based geopolymer and the influence of calcium compounds that form CSH type of phase can also be neglected. Therefore, it can be assumed that the geopolymeric type of phase was formed in the milled samples preferentially than in the raw sample. The compressive strength of the attrition milled fly ash based geopolymer was 20% higher than vibration milled fly ash based geopolymer. Kumar and Kumar [9] observed that the compressive strength of the geopolymer specimens increases with reduction of the average particle size ( $D_{50}$ ) after milling. They suggested that the particle





**Figure 5:** High and low magnification SEM micrographs of the raw fly ash (A, B), attrition milled (C,D) and vibration milled (E, F) fly ash based geopolymers.

size has an important effect on strength development. The same behaviour was observed at present case.

Generally the microstructure of the alkali-activated materials is consistent with the mechanical properties data. This is also the case here observing the SEM micro-

graphs of the geopolymers prepared from raw and milled fly ashes (Figure 5).

The attrition milled fly ash based geopolymer showed denser microstructure than vibration milled or raw fly ash based geopolymers. Mechanical activation enhances geopolymerization reaction, which is apparently depend

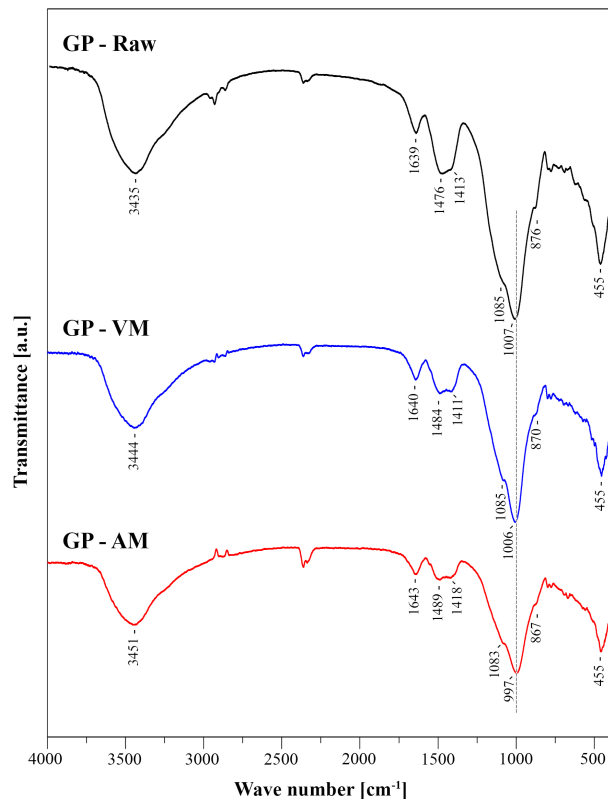


**Figure 6:** FTIR spectra of geopolymers prepared from raw and milled fly ashes.

on microstructural changes of the milled fly ashes. Generally the milling could cause weakening of specific bonds within the fly ash including the important bonds for alkali activated materials such as Si-O-Al, Si-O-Si and Al-O-Al. Weakened bonds are susceptible to alkali activation and easily reacts with  $(\text{OH})^-$ . Rapture of the aluminosilicate bonds and formation of amorphous structure is well described in mechanically activated kaolinite [24]. On the other hand, milling not only caused decrease of the particle sizes of the powders but also formation of the aluminosilicate (Si-O-Al) bonds between the aluminate and silicate sources and improved homogeneity [25]. In contrast to the materials used for mullite precursors [25], the fly ash has a more complex composition with amorphous and crystalline constituents and usually the crystalline part embedded within a glass matrix. The chemical composition also varies. It contains aluminosilicates with crystalline and amorphous compositions as well as aluminate and silicate as separated constituents. Therefore, strong vibration milling not only weakens microstructure of certain components and enhance their reactivity, but also may lead to the formation of new aluminosilicate bonds between aluminate and silicate constituents of the fly ash

as it caused more microstructural changes. Kanuchova *et al.* [26] have observed an increase in binding energy with the appearance of new specifications for Al and Si atoms by XPS method in mechanically activated fly ash. Such changes of the binding energy indicate the appearance of new Al-O-Si bonds.

The strengths of the Al-O and Si-O bonds are 511 kJ/mol and 799 kJ/mol, respectively. Consequently, the aluminium source dissolves in alkaline medium faster than the silica source [27]. Within the Si-O-Al sialate units the strength of the Al-O bond is suggested to be higher compared to a single Al-O bond. Although, at present, there is no evidence on possible mechanochemical Al-O-Si bond formation in the vibration milled fly ash we suggest that it could be the reason of lower compressive strength of vibration milled fly ash based geopolymer, because of weaker dissolution of the aluminate and silicate units in the alkaline liquid. The formation of new relative stable geopolymer type units favourably influenced by the increased content of smaller sized particles without heavily structural distortion for attrition milled fly ash compared to the vibration milled samples (Figure 1). Moreover, the formation of poly-sialate units is favoured in alkaline solution as could be adapted from the alkaline and acidic leaching experiments of zeolite X and Y [28]. Also the additional TG-loss observed for the vibration milled samples may indicated a significant formation of OH-group, e.g. of type  $\text{AlOOH}$ ,  $\text{Al}(\text{OH})_3$  which makes an alkali activation of the material less effective.

Figure 6 shows FTIR spectra of the geopolymers prepared from raw, vibration and attrition milled fly ashes. There are the main peaks at around 3450, 1640, 1485, 1415, 1085, 997, 870 and 455  $\text{cm}^{-1}$ . In contrast to unreacted fly ashes in Figure 4 the geopolymerized fly ash shows shift of the 1087  $\text{cm}^{-1}$  peak to 997  $\text{cm}^{-1}$ , 1006  $\text{cm}^{-1}$  and 1008  $\text{cm}^{-1}$  for the attrition milled, vibration milled and raw fly ash based geopolymers, respectively. The Si-O-Si bond due to amorphous silica appearing at about 1070-1100  $\text{cm}^{-1}$  shifts to lower wave number due to structural re-organization and formation of Al-O-Si bond in the geopolymer structure [15]. The band at 1096  $\text{cm}^{-1}$  that initially appeared in the unreacted fly ash (Figure 4) becomes split and the main peak shifted to 1000  $\text{cm}^{-1}$ . Characteristic band due to Si-O-Al bond formation in the geopolymer at around 1000  $\text{cm}^{-1}$  has highest shift from the starting fly ash in the attrition milled fly ash based geopolymers followed by vibration and raw fly ashes. It can be suggested that the Si-O-Al bond was formed more preferentially in the attrition milled fly ash and it has a higher content of geopolymer.

Peaks at 3450 and 1640  $\text{cm}^{-1}$  are assigned to -OH, HOH bonds of hydroxyl groups and free water. There are 2 types



of carbonate peaks at 1489, 1415 and 870  $\text{cm}^{-1}$ . Peaks at 1489 and 870  $\text{cm}^{-1}$  are assigned to calcium carbonate such as vaterite ( $\text{CaCO}_3$ ) [29], while peak at 1415  $\text{cm}^{-1}$  assigned to sodium carbonate. The bands at 1085 and 455  $\text{cm}^{-1}$  are assigned to Si-O vibration of the silica.

Figure 7 shows XRD patterns of geopolymer samples prepared from the raw and milled fly ashes. Diffraction pattern of the raw fly ash is inserted for comparison. Interestingly in the raw and vibration milled fly ash based geopolymers were observed some small intensity peaks denoted as  $X_{1234}$  and  $X_5$ . It could indicate appearance of zeolite type and Na-Si-Ca-Al silicate hydrate type phases. The attrition milled fly ash based geopolymer showed slightly larger amorphous and significantly less crystalline intensity compared to the vibration milled fly ash based geopolymer as indicated in the appropriate difference pattern. The X-ray amorphous geopolymer phase is typically indicated by a broad peak centred around  $28\text{--}30^\circ 2\theta$ . It may be suggested, that the presence of crystalline phases are not beneficial for a better mechanical strength here.

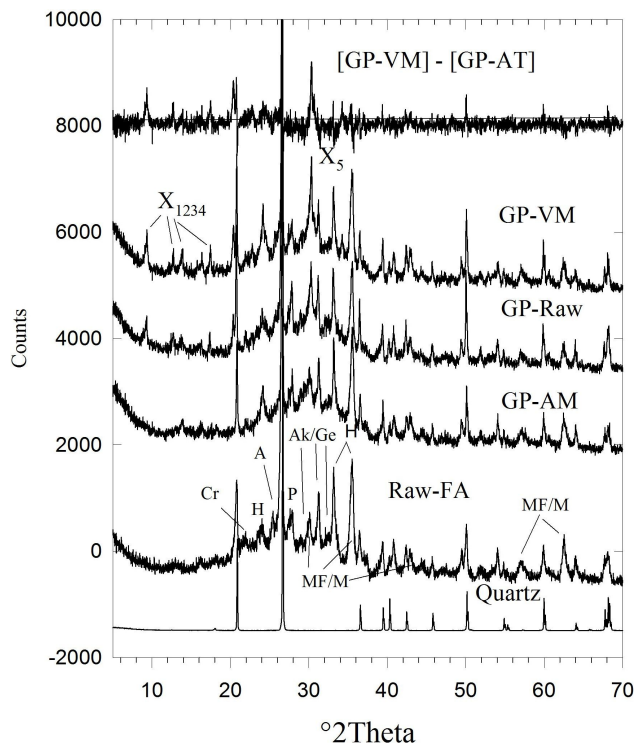


**Figure 7:** XRD patterns of raw fly ash (Fa-raw) and geopolymer samples prepared from raw and milled fly ashes, GP-AT (attrition milled), GP-FA-raw (raw fly ash used), GP-VM (vibration milled). Identification: Cr = Crisobalite, H = Hematite, A = Anhydrite, P = Plagioclase, Ak/Ge = Akermanite/Gehlinite, MF/M = Magnesioferrite/Magnetite, Quartz,  $X_{1234}$ ,  $X_5$  = Additional peaks seen only for GP-VM and GP-FA-raw. [GP-VM]-[GP-AT] denotes the difference pattern.

The present research supports the conclusion by Mucsi *et al.* [13] on beneficial influence of attrition mill over the vibration mill for fly ash grinding. The attrition mill is more suitable milling device for preparation of geopolymers from high calcium fly ash. Energy efficiency of attrition mill in comparison to vibration mill is obvious, as it previously for stirred media ball [13]. They have shown that specific grinding energy (kJ/kg) requirement for reducing the same particle size for vibration mill at least 10 times higher than that of for stirred media mill. Our research shows that regardless used raw materials type the attrition mill is more suitable device in terms of both energy efficiency and improved reactivity of milled fly ash to alkaline liquid.

## 5 Conclusions

The mechanical properties of the geopolymers prepared using fly ash from 4<sup>th</sup> Thermal power station of Ulaanbaatar city are improved using attrition milled fly ash over vibration milled fly ash. The particle size reduction rate for attrition and vibration milling was almost identical. With the same milling efficiency criteria, the attrition mill is a more suitable milling device for mechanical activation of fly ash for further alkali activation than vibration mill. High efficiency of the attrition mill for fly ash activation is related with the decrease in particle size without heavily distortion of microstructure. However, in the vibration milled fly ash could occur mechanochemical reaction by formation of the new chemical bonds. Such homogenized structure shows the negative influence on reactivity of fly ash expressed by geopolymerization reaction.

**Acknowledgement:** The present research was supported by the Korea-Mongolian joint project (15RDRPB103390-03) “Development of Energetically Modified Materials and Mortar-Concrete Using EMC and ceramic fiber”, the Korea Ministry of Land, Infrastructure, and Transport. Support from the Mongolian foundation for Science and Technology and Alexander von Humboldt Foundation (Germany) is also acknowledged.

## References

- [1] R. S. Blissett and N. A. Rowson, *Fuel*, 97 (2012) 1-23.
- [2] P. Asokan, M. Saxena, and S. R. Asolekar, *Res. Conserv. Recycl.*, 43 (2005) 239-262.
- [3] M. Ahmaruzzaman, *Prog. Ener. Combust. Sci.*, 36 (2010) 327-363.

- [4] J. L. Provis and J. S. J. van Deventer (Eds.), *Alkali Activated Materials, State-of-the-Art Report*. RILEM TC 224-AAM, London, Springer, (2014), p. 388.
- [5] J. T. Gourley, *J. Aus. Ceram. Soc.*, 50 (2014) 102-110.
- [6] A. Kumar, R. Kumar, T. C. Alex, A. Bandopadhyay, and S. P. Melhotra, *Advance. in Appl. Cer.*, 106 (2007) 120-127.
- [7] M. Erdemoglu and P. Balaz, *Min. Process. and Extractive Metall. Rev.* 33 (2012) 65-88.
- [8] S. Kumar, R. Kumar, and S. P. Mehrotra, In: *INCOME2008 Proceedings, Frontiers in Mechanochemistry and Mechanical Alloying*, pp.320-323.
- [9] S. Kumar and R. Kumar, *Ceram. Int.*, 37 (2011) 533-541.
- [10] R. Kumar, S. Kumar, and S. P. Melhotra, *Res. Conserv. Recycl.* 52 (2007) 157-179.
- [11] P. Balaz, *Mechanochemistry in Nanoscience and Minerals Engineering*, Springer, Berlin-Heidelberg, (2008).
- [12] P. Balaz, *Extractive metallurgy of activated minerals*, Elsevier, Amsterdam, (2000), p.278.
- [13] G. Mucsi, S. Kumar, B. Csoke, R. Kumar, Z. Molnar, A. Racz, et al., *Int. J. Min.Proc.*, 143 (2015) 50-58.
- [14] J. Temuujin, A. Minjigmaa, U. Bayarzul, D. S. Kim, S. H. Lee, H. J. Lee, et al., *Materiales de construcción*, 67 (2017) e134.
- [15] J. Temuujin, A. Minjigmaa, B. Davaabal, U. Bayarzul, A. Ankhtuya, Ts. Jadambaa, et al., *Cer. Inter.* 40 (2014) 16475-16483.
- [16] J. Temuujin, E. Surenjav, C. H. Ruescher, and J. Vahlbruch, *Chemosphere*, 216 (2019) 866-882.
- [17] C. Papastefanou, *J. Environ. Radioactivity*, 101 (2010) 191-200.
- [18] M. Fan and R. C. Brown, *Energy.Fuels.*, 15 (2001) 1414-1417.
- [19] W. Mozgawa, M. Krol, J. Dyczek, and J. Deja, *Spectrochim. Acta Part A: Molecul. Biomolecul. Spectroscopy*, 132 (2014) 889-894.
- [20] E. Ryshkewitch, *J Am. Cer. Soc.*, 36 (1953) 65-68.
- [21] K. K. Schiller, *Cem. Concr. Res.*, 1 (1971) 419-422.
- [22] J. J. Beaudoin and V. S. Ramachandran, *Cem. Concr. Res.* 22 (1992) 689-694.
- [23] J. Temuujin, A. Minjigmaa, W. Rickard, and A. Van Riessen, *J. Therm. Analys. Calor.*, 107 (2012) 287-292.
- [24] S. Kawai, M. Yoshida, and G. Hashizume, *J. Ceram. Soc. Jpn.*, 98 (1990) 669-674.
- [25] J. Temuujin, K. Okada, and K. J. D. MacKenzie, *J. Mat. Res.*, 13 (1998) 2184-2189.
- [26] M. Kanuchova, M. Drabova, M. Sisol, J. Mosej, L. Kozakova, and J. Skvarla, *Env. Prog. Sustainable Energ.*, 35 (2018) 1338-1343.
- [27] Y.R. Luo, *Comprehensive handbook of Chemical bond energies*, CRC Press, Boca Raton, (2007).
- [28] W. Lutz, C. H. Rüscher, and D. Heidemann, *Micropor. Mesop. Mat.*, 55 (2002) 193-202.
- [29] M. Sato and S. Matsuda, *Zeitschrift fuer Kristallograph.*, 129 (1969) 405-410.